Elsevier Editorial System(tm) for Radiation Measurements
Manuscript Draft

Manuscript Number: RADMEAS-D-15-00285R2

Title: An approach to discriminatively determine thoron and radon emanation rates for a granular material with a scintillation cell

Article Type: Full Length Article

Keywords: Thoron; Radon; Emanation; Sandwich technique; Granular materials; Scintillation cell

Corresponding Author: Dr. Akihiro Sakoda,

Corresponding Author's Institution: Japan Atomic Energy Agency

First Author: Akihiro Sakoda

Order of Authors: Akihiro Sakoda; Oliver Meisenberg; Jochen Tschiersch

Abstract: A powder sandwich technique was applied to determine thoron (220Rn) and radon (222Rn) emanation rates for a granular material. The feature of this technique is the sample preparation, in which a granular material is put and fixed between two membrane filters. Airflow is directly given to this sandwich sample, will include thoron and radon emanated from the material, and then is transferred to the detector. This method makes sure that radon as well as thoron emanated is not retained in pore space within the sample volume, which is crucial for the appropriate emanation test. This technique was first introduced by Kanse et al. (2013) with the intention to measure the emanation of thoron - but not of radon - from materials having much higher 224Ra activity than 226Ra. In the present study, the methodology for the discriminative determination of thoron and radon emanation rates from a granular material has been examined using a flow-through scintillation cell and sandwich sample. The mathematical model was developed to differentiate total alpha counts into thoron- and radon-associated counts. With a sample of uranium ore, this model was experimentally validated by comparison between the scintillation cell and a reference detector that can discriminatively measure thoron and radon concentrations. Furthermore, the detection limits and uncertainties were evaluated to discuss the characteristics of this method. Key parameters for their improvement were found to be the background radon concentration and the leakage of radon from the measurement system, respectively. It was concluded that the present method is advantageous to a sample that has much higher 226Ra activity than 224Ra if the emanation fractions are similar between thoron and radon.

Dr. Bailiff
Editor-in-Chief, Radiation Measurements

January 20, 2016

Dear Dr. Bailiff,

We would like to submit the revised manuscript to Radiation Measurements.

- Type: Full-length paper
- Title: An approach to discriminatively determine thoron and radon emanation rates for a granular material with a scintillation cell
- Authors: Akihiro Sakoda, Oliver Meisenberg, Jochen Tschiersch
- This manuscript has been approved by all authors.
  - –Texts 20 (including the Title page and Figure captions)
  - –Figures 4
  - –Table 3

We appreciate your careful review and kind consideration of our manuscript. The manuscript has been revised based on the comments. We hope that this submission is meeting the requirement of Radiation Measurements. We are looking forward to hearing from you.

Yours sincerely,

Akihiro Sakoda, Ph.D.
Japan Atomic Energy Agency,
1550 Kamisaibara, Kagamino-cho, Tomata-gun,
Okayama, 708-0698, Japan
Tel: +81-868-44-2211
Fax: +81-868-44-2851
E-mail: sakoda.akihiro@jaea.go.jp

Associate editor

Comment #1:

Please at least include the reference to the Falk paper (see comments on the original manuscript) to give some perspective on how scintillation cells can be used for combined radon-220 and randon-222 measurements.

Response #1:

The revised manuscript refers to the Falk's paper to mention the thoron and randon measurement using a scintillation cell. The following was added into the Introduction section (lines 3-9 from the bottom in the last paragraph).

" Although there are some methods for this discrimination (e.g. so-called coincidence technique (Falk et al., 1992)), the present work developed a mathematical model to differentiate total alpha counts into thoron- and radon-associated counts. This approach seemed simpler and was expected to work well for the emanation test, as long as all parameters used for the model formulae were known. The present model was experimentally validated by comparing the differentiated counts with radon and thoron data given by a reference detector. "

Comment #2:

Please correct the problem with the "world-average" radon-220 and radon-222 sample-specific emanation rates in Fig. 4. One solution is to clarify (in the figure caption and/or on the x-axis) that the data are specific for a 2 g sample size. Furthermore, would have to rename the "world average" to "reference value" or something like that and then write in the caption that the indicated reference values were calculated for the 2 g sample size using world average values for radium concentrations and emanation fractions as indicated in the text.

Response #2:

According to your suggestion, we renamed the "world average" to "reference value", and then clarified in the figure caption that the reference values were corresponding to the emanation rate from a 2-g sample with world average values for radium concentrations and emanation fractions as indicated in the text. Please see Fig. 4 and its caption.

[Fig. 4 Caption]

“ Expected relative uncertainties of thoron and radon emanation rates measured by the present method. The details of the experimental conditions are given in Table 2. The indicated reference values were calculated for the sample mass 2 g, which was typical for the dimension of the applied sandwich sample, using the world averages of radium concentrations and thoron and radon emanation fractions as indicated in the text. ”

Highlights for "An approach to discriminatively determine thoron and radon emanation rates for a granular material with a scintillation cell"

• The methodology of appropriate and discriminative measurement of thoron and radon emanation is presented.

• Measurement of thoron and radon emanating from a sample was made using a scintillation cell.

• Detection limits and uncertainties were estimated in detail to characterize the present method.

• The advantage of the present technique is given especially to a sample having much higher ^{226}Ra activity than ^{224}Ra.

Regular paper:

An approach to discriminatively determine thoron and radon emanation rates for a granular material with a scintillation cell

Akihiro Sakoda[1,2], Oliver Meisenberg[2,*], Jochen Tschiersch[2]

[1] Ningyo-toge Environmental Engineering Center, Japan Atomic Energy Agency, 1550 Kamisaibara, Kagamino-cho, Tomata-gun, Okayama 708-0698, Japan

[2] Helmholtz Zentrum München, German Research Center for Environmental Health, Institute of Radiation Protection, Ingolstädter Landstr. 1, 85764 Neuherberg, Germany

[*] Present address: Federal Office for Radiation Protection, Ingolstädter Landstr. 1, 85764 Neuherberg, Germany

Corresponding author: Akihiro Sakoda

Tel: +81-868-44-2211

Fax: +81-868-44-2851

E-mail: sakoda.akihiro@jaea.go.jp

Abstract

A powder sandwich technique was applied to determine thoron (^{220}Rn) and radon (^{222}Rn) emanation rates for a granular material. The feature of this technique is the sample preparation, in which a granular material is put and fixed between two membrane filters. Airflow is directly given to this sandwich sample, will include thoron and radon emanated from the material, and then is transferred to the detector. This method makes sure that radon as well as thoron emanated is not retained in pore space within the sample volume, which is crucial for the appropriate emanation test. This technique was first introduced by Kanse et al. (2013) with the intention to measure the emanation of thoron - but not of radon - from materials having much higher ^{224}Ra activity than ^{226}Ra. In the present study, the methodology for the discriminative determination of thoron and radon emanation rates from a granular material has been examined using a flow-through scintillation cell and sandwich sample. The mathematical model was developed to differentiate total alpha counts into thoron- and radon-associated counts. With a sample of uranium ore, this model was experimentally validated by comparison between the scintillation cell and a reference detector that can discriminatively measure thoron and radon concentrations. Furthermore, the detection limits and uncertainties were evaluated to discuss the characteristics of this method. Key parameters for their improvement were found to be the background radon concentration and the leakage of radon from the measurement system, respectively. It was concluded

that the present method is advantageous to a sample that has much higher ^{226}Ra activity than ^{224}Ra if the emanation fractions are similar between thoron and radon.

Keywords: Thoron; Radon; Emanation; Sandwich technique; Granular materials; Scintillation cell

1. Introduction

In addition to radon (^{222}Rn), attention has recently been focused on thoron (^{220}Rn) from the standpoint of radiation protection. In spite of its short half-life of 55.8 s, thoron concentration in dwellings is known to be elevated depending on building materials (Reddy et al., 2004; Tokonami et al., 2004; Gierl et al., 2014). Unfired earthen materials have been found to yield high thoron concentration. In this context, it seems important to understand thoron emanation from various materials, but its relevant reports are much fewer than those on radon (IAEA, 2013). Emanation of radon or thoron is defined as escape of its atom from a Ra-bearing material grain into pore space.

Recently, Kanse et al. (2013) reported a unique sample preparation for the emanation test, called “powder sandwich technique”. However, their method was dedicated to only thoron and not to radon. A powder material was sandwiched with a thickness of a few millimeters by using two membrane filters. Airflow directly given to this sandwich sample will include thoron and radon emanated from the material, and then it is introduced to the detector. Thus, it can be assured that thoron (and also radon) emanated from the material is not retained in pore space in the volume of the bulk sample. Whereas this retention had been considered to be one of the most crucial problems for conventional emanation measurements (e.g. so-called accumulation method, which uses an airtight chamber where a sample material is placed (see Sakoda et al. (2008)), the sandwich technique was expected to readily solve this problem. If the accumulation method is employed for the emanation measurement, the thickness of the sample must be as thin as possible because thoron and radon should instantaneously diffuse out of the volume of the bulk sample so that their concentrations are uniform in the chamber including the pore spaces of the sample. Otherwise, the measured result should be regarded as the *exhalation* rate rather than the *emanation*: the exhalation process includes the emanation and its subsequent transport along pores (Sakoda et al., 2011; IAEA, 2013).

In the present paper, expanding the work of Kanse et al. (2013), we propose a methodology to discriminatively determine thoron and radon emanation rates from a granular material using a flow-through scintillation cell and sandwich sample. This detector has a simple structure, and basically requires no accessory like desiccant (Lucas, 1957). In general, however, its detector system can only detect alpha particles emitted in the cell, and does not discriminate them: namely it provides no information on the kind of radionuclide. Although there are some methods for this discrimination (e.g. so-called coincidence technique (Falk et al., 1992)), the present work developed a mathematical model to differentiate total alpha counts into thoron- and radon-associated counts. This approach seemed simpler and was expected to work well for the emanation test, as long as all parameters used for the model formulae were known. The present model was experimentally validated by comparing the differentiated counts with radon and thoron data given by a reference detector. Moreover, the detection limits and uncertainties were evaluated to know the limitation of the present method, and its advantages were also discussed.

2. Materials and methods

A thin cylindrical sample (diameter 4.1 cm; thickness 0.25 cm), which was composed of a granular material sandwiched by two PTFE (polytetrafluorethylen) filters, was made as shown in Fig. 1 (a). This sandwich sample was set in the closed measurement system (Fig. 1 (b)), which consisted of a glass microfiber filter as a backup filter, inlet filter, flow-rate adjustable pump, scintillation cell (300A, PYLON, Canada) and its radiation monitor (AB-5, PYLON, Canada).

At the same time as switching on the pump, counting of alpha particles from thoron, ^{216}Po, ^{212}Bi, ^{212}Po, radon, ^{218}Po and ^{214}Po was started and continued for some days. The contribution from ^{210}Po, which is a progeny of ^{210}Pb with the long half-life of 22.23 y, was ignored for the subsequent analytical treatment. The measurement period was fixed based on the buildup curve of the alpha counts. Here, the material examined should be kept under the environmental condition of interest before and during the measurement, because the emanation power is sensitive to parameters like moisture content (reviewed by Sakoda et al., 2011). The flow rate should be less than 0.5 l min^{-1} to assure the radioactive equilibrium between thoron and ^{216}Po in the flow-through scintillation cell. The ratio of ^{216}Po activity to thoron can be calculated to be 0.996 at the flow rate of 0.5 l min^{-1}, assuming that ^{216}Po is not deposited on the cell wall due to its very short half-life (0.150 s). The discharge fractions of other thoron and radon progenies, which were not deposited on the cell wall, from the flow-through cell were estimated using our empirical data (Sakoda et al., 2015), and were used for implementing a mathematical model as explained below.

A mathematical model to predict activities of thoron, radon and their progenies in the scintillation cell was developed, which is indicated in Table 1. The behaviors of the nuclides were formulated separately for their location in the cell volume or on the wall, since the detection efficiencies of alpha particles emitted are different between the two locations. The set of differential equations in Table 1 was analytically solved, and then the activity for each nuclide was integrated over a certain counting interval (one hour in the case of Fig. 2 (a)). Here, it is noted that for ^{212}Bi, the activity was restricted to that related to alpha decay. Alpha counts can be acquired by multiplying the integrated activity by the corresponding detection efficiency. Consequently, counts ($C_{\mathrm{i,n}}$ (-)) per counting cycle (t (s)) is expressed as:

(1) Thoron series

$$C_{\mathrm{Tn}}(t) = C_{\mathrm{c,Rn\text{-}220}}(t) + C_{\mathrm{c,Po\text{-}216}}(t) + C_{\mathrm{w,Bi\text{-}212}}(t) + C_{\mathrm{w,Po\text{-}212}}(t), \quad (1)$$

(2) Radon series

$$C_{\mathrm{Rn}}(t) = C_{\mathrm{c,Rn\text{-}222}}(t) + C_{\mathrm{c,Po\text{-}218}}(t) + C_{\mathrm{w,Po\text{-}218}}(t) + C_{\mathrm{w,Po\text{-}214}}(t), \quad (2)$$

and

(3) Total counts

$$C(t) = C_{\mathrm{Tn}}(t) + C_{\mathrm{Rn}}(t), \quad (3)$$

where the subscript, i, indicates the location of the nuclide (c: in the cell volume, and w: on the wall), and the subscript, n, the nuclide. Finally, Eq. 3 was fitted to a set of measured data over all counting cycles to estimate unknown parameters, i.e. thoron and radon emanation rates (R (Bq s^{-1})) and leakage rate (α (s^{-1})) of radon from the measurement system. The thoron or radon emanation fraction (F (-)) is written as:

$$F = \frac{R}{\lambda S W}, \tag{4}$$

where λ (s^{-1}) is the decay constant of thoron or radon, S (Bq kg^{-1}) the ^{224}Ra or ^{226}Ra concentration in the sample material, and W (kg) the sample mass. The parameter F is not further mentioned in this paper because R is of particular interest.

In order to validate the present methodology, an instrument which can separately measure thoron and radon concentrations in principle was prepared as a reference. The device commercially called RAD7 (DURRIDGE, USA), which can determine both thoron and radon concentrations based on alpha-ray spectrometry, was used for this purpose. The comparison tests were carried out between the scintillation cell and RAD7 for thoron and radon emanation rates from a crushed uranium ore (0.7 g). Since RAD7 requires the usage of desiccant and the measurement system was closed, the relative humidity in the system was low (ca. 5%). Thus, the emanation test using the scintillation cell was also performed under the same level of humidity as well as temperature. The analysis of the buildup of thoron and radon concentrations provided by RAD7 to obtain thoron and radon emanation rates from the sample was basically in accordance with

Kanse et al. (2013) for thoron and Sakoda et al. (2008) for radon. Measurement uncertainty (coverage factor k=1) was estimated by the Monte Carlo method (JCGM, 2008).

3. Results and discussion

Figure 2 shows the comparison of the thoron and radon emanation rates from the crushed uranium ore measured with the scintillation cell and RAD7. The open and closed circles are raw data provided by the devices. In Fig. 2 (a), the curves of “Thoron” and “Radon” were obtained by fitting Eq. 3 to the measured data: the sum of the “Thoron” and “Radon” curves is identical to the “Total”. In Fig. 2 (b), the fitting curves were acquired from the thoron or radon concentration measured with RAD7. It is obvious that the values of the thoron and radon emanation are in a good agreement between the two devices. This suggests that the model of Table 1 is reasonable and available for the quantification of the emanation rates using the flow-through scintillation cell. The difference in the trends of the two curves for thoron in Figs. 2 (a) and (b) can be seen: there is a gradual increase of counts only in the usage of the scintillation cell. This is due to the accumulation of ^{212}Pb and its progeny on the cell wall with time. Time needed for the radioactive equilibrium between ^{224}Ra and thoron or ^{212}Pb is about 10 min or 5 d, respectively. Thus, the thoron concentrations measured with RAD7, which can directly output its concentrations that were corrected for the buildup of the progeny, became stable quickly.

The application of the system using the sandwich sample is simple and easy (Fig. 1), and is expected to work well for any environment. If an emanation test is carried out under a natural room condition, a scintillation cell is one of the most suitable detectors because no desired accessory may influence the conditions. For example, the incorporation of desiccant, which is required by RAD7, results in the significant reduction of humidity, if the closed system volume is not so large. On the other hand, if environmental parameters are arbitrarily changed to study their effects on emanation, the current system must be modified. Nevertheless, the methodology mentioned in this paper would be useful and valuable as far as its limitation and advantage are understood as described later. It is noteworthy that the present method ensures the accurate emanation determination for the material according to the definition of *emanation* (see the Introduction section).

Next, the detection limits in the present method are discussed, which were estimated by Monte Carlo simulation as follows. The series of alpha counts with time was first theoretically made by the model shown in Table 1 with the parameters randomly selected based on their uncertainties. The different mean values of the parameters listed in Table 2 were applied, taking into consideration the common condition seen in the present experiment ("Original" in the table) and other modified conditions. The individual detection efficiencies of alpha emitters for the discrimination level of 1.2 or

4.0 MeV are exhibited in Table 3. The measurement period was assumed to be five days. Subsequently, the theoretically obtained counts were randomized by a Poisson distribution to simulate the fluctuation of counts. The randomized counts were fitted using the same model and parameters considering their uncertainties, and then the thoron and radon emanation rates were determined (although their real values were known in this case). The set of these procedures was repeated enough to obtain the means and uncertainties (standard deviations) of the thoron and radon emanation rates. In this work, a 5% false-negative possibility was chosen as an acceptance level for the decision of the detection limit.

For implementing this computation, a co-existing radon or thoron emanation rate for the isotope which is out of interest for the moment (hereafter called as “co-emanation”) must be assumed. For the detection limit of the thoron emanation rate, the emanation of radon causes a kind of background counts having a predictable time trend, which are regarded as co-emanation. On the other hand, for the detection limit of the radon emanation rate, the emanation of thoron causes background counts, which are regarded as co-emanation in this case. Obviously, background is one of the most important factors to govern the detection limit. The co-emanation rates (2.7×10^{-8} Bq s^{-1} for radon and 1.6×10^{-4} Bq s^{-1} for thoron) were set on the assumption of the sample mass of 2 g, which is typical for the dimension of the sandwich sample shown in Fig. 1 (a), and the worldwide averages of radium concentrations and radon and thoron emanation fractions: 32 Bq kg^{-1} for ^{226}Ra, 45 Bq kg^{-1} for ^{224}Ra (UNSCEAR, 2010), 0.2 for radon (Sakoda et al., 2011), and 0.14 for thoron (IAEA, 2013). The co-emanation rate can be calculated by multiplying the product of these three parameters with the decay constant of radon or thoron. Furthermore, two other co-emanation rates, which were 10 and 100 times higher than the above values, were also assumed.

Table 2 implies that the most effective parameters for improving the detection limits of thoron and radon emanation rates are the background radon concentration ($C_{\mathrm{BG,Rn\text{-}222}}$) and the leakage rate of radon (α), respectively. The magnitude of the impact of this parameter was about four times greater for thoron $((7.9\times10^{-5})/(4.9\times10^{-6})=16)$ than radon $((6.1\times10^{-8})/(1.7\times10^{-8})=3.6)$. The results for the condition 5-1 to 5-3 show that the increase of the thoron co-emanation rate has larger interference with the determination of the radon emanation rate. The hundredfold increases of the radon and thoron co-emanations made worse the detection limits of the thoron and radon emanation rates by factors of about 1.6 $(=(4.7\times10^{-5})/(2.9\times10^{-5}))$ and 24 $(=(4.7\times10^{-7})/(2.0\times10^{-8}))$, respectively. Figure 3 shows the theoretical calculation of the buildup curves of counts with time after starting the measurement, indicating that alpha counts from thoron and its progeny are much larger than those from radon when ^{224}Ra and ^{226}Ra activities are similar and there is a detectable leakage of radon from the measurement system. Thus, it can be understood that the random fluctuation of the thoron-associated counts can more easily influence the curve fitting for the radon emanation rate than the other way round. This argument also leads to the fact, as already mentioned, that it is most important to minimize the leakage of radon and gain its associated counts in order to improve the detection limit of the radon emanation rate. On the other hand, the thoron emanation rate can be determined from data of the first few counting intervals, where the background counts from radon and its progeny mainly interfere with the curve fitting for the thoron emanation rate. Hence, the implication of Table 2, as mentioned above, seems to be reasonable that the key parameter for the detection limit of the thoron emanation rate is the background radon concentration.

If the measured emanation rates are beyond the detection limits, it becomes necessary to evaluate the uncertainties (standard deviations). It is next discussed how the measurement uncertainty depends on experimental parameters specified in Table 2. The uncertainties for different parameter values were computed by the same procedures of Monte Carlo simulation which were employed for the estimation of the detection limits. However, the series of alpha counts with time that was theoretically made by the model of Table 1 was based on the mean values of the parameters without considering their uncertainties. Figure 4 shows the relationship between the thoron or radon emanation rate and its relative uncertainty. It is clear that the relative uncertainty decreases with increasing the emanation rate, and that the experimental condition having the lower detection limit approximates the minimum of relative uncertainties at lower emanation rate. The vertical dashed lines in the figure represent the reference emanation values. For a common sample which has 1.6×10^{-4} for thoron and 2.7×10^{-8} Bq s^{-1} for radon (Condition 1 to 4), thoron emanation rates can be determined within the range of 9-24% (Fig. 4 (a)). Also, such radon emanation rates can be quantified with a relative uncertainty of 29% at best, and some experimental conditions cannot determine them (Fig. 4 (b)). These results mean that the present method allow us to better evaluate emanation rates of thoron than of radon. On the other hand, in the condition 5-1 to 5-3, even though the thoron or radon co-emanation rate becomes 10 or 100 times larger, the shift of the curve to the right side (larger emanation-rate side) is much less than one or two orders of magnitude, respectively. This suggests that the sample preparation with larger mass results in improving not only the detection limit but also the uncertainty of the emanation rate.

Based on the above discussion, it can be concluded that the advantage of the present method is given especially to a sample that includes much higher ^{226}Ra activity than ^{224}Ra, if the emanation fractions are similar for both thoron and radon: for example, uranium mill tailings and uranium ores. In the opposite situation as $^{226}Ra \ll {}^{224}Ra$, the measured radon emanation rate could be ignored as Kanse et al. (2013) or should carefully be treated, whereas the thoron emanation rate is expected to be determined accurately. This is because much larger counts from thoron and its progeny are expected from Fig. 3, and will make it hard to observe alpha counts from radon and its progeny by curve fitting and quantify the radon emanation rate.

4. Conclusions

The methodology to discriminatively quantify thoron and radon emanation rates for a granular sample using a scintillation cell was presented. It was experimentally validated, which implies that the developed mathematical model was working well. The detection limits and uncertainties of thoron and radon emanation rates were also discussed in detail. As a result, the background radon concentration and leakage rate of radon from the system were identified as important parameters to improve the determination of thoron and radon emanations, respectively. It was then stated that a sample with higher ^{226}Ra than ^{224}Ra is preferable for the present method.

The feature of the present method was the sample preparation (called sandwich technique), and the sample thickness was a few millimeters. We believe that this technique ensures appropriate emanation measurements according to the definition of emanation, since the present method does not depend on the diffusion process of thoron and radon from pore space of the sample into free air space in the system. Only thoron and radon released into such free space have a chance to be detected by the detector.

References

Falk, R., Möre, H., Nyblom, L., 1992. Measuring techniques for environmental levels of radon-220 in air using flow-through Lucas cell and multiple time analysis of recorded pulse events. Appl. Radiat. Isot. 43, 111-118.

Gierl, S., Meisenberg, O., Feistenauer, P., Tschiersch, J., 2014. Thoron and thoron progeny measurements in German clay houses. Radiat. Prot. Dosim. 160, 160-163.

International Atomic Energy Agency (IAEA), 2013. Measurement and Calculation of Radon Releases from NORM Residues. Technical Reports Series No. 474. IAEA, Vienna.

Joint Committee for Guides in Metrology (JCGM), 2008. Evaluation of Measurement Data - Supplement 1 to the Guide to the Expression of Uncertainty in Measurement Propagation of Distributions Using a Monte Carlo Method. JCGM 101: 2008.

Kanse, S.D., Sahoo, B.K., Sapra, B.K., Gaware, J.J., Mayya, Y.S., 2013. Powder sandwich technique: A novel method for determining the thoron emanation potential of powders bearing high ^{224}Ra content. Radiat. Meas. 48, 82-87.

Lucas, H.F., 1957. Improved low-level alpha-scintillation counter for radon. Rev. Sci. instrum. 28, 680-683.

Reddy, M.S., Reddy, P.Y., Reddy, K.R., Eappen, K.P., Ramachandran, T.V., Mayya, Y.S., 2004. Thoron levels in the dwellings of Hyderabad city, Andhra Pradesh, India. J. Environ. Radioact. 73, 21-28.

Sakoda, A., Hanamoto, K., Ishimori, Y., Nagamatsu, T., Yamaoka, K., 2008. Radioactivity and radon emanation fraction of the granites sampled at Misasa and Badgastein. Appl. Radiat. Isot. 66, 648-652.

Sakoda, A., Ishimori, Y., Yamaoka, K., 2011. A comprehensive review of radon emanation measurements for mineral, rock, soil, mill tailing and fly ash. Appl. Radiat. Isot. 69, 1422-1435.

Sakoda, A., Meisenberg, O., Tschiersch, J., 2015. Behavior of radon progeny produced in a scintillation cell in the flow-through condition. Radiat. Meas. 77, 41-45.

Tokonami, S., Sun, Q., Akiba, S., Zhuo, W., Furukawa, M., Ishikawa, T., Hou, C., Zhang, S., Narazaki, Y., Ohji, B., Yonehara, H., Yamada, Y., 2004. Radon and thoron exposures for cave residents in Shanxi and Shaanxi provinces. Radiat. Res. 162, 390-396.

Tokonami, S., Yang, M., Yonehara, H., Yamada, Y., 2002. Simple, discriminative measurement technique for radon and thoron concentrations with a single scintillation cell. Rev. Sci. instrum. 73, 69-72.

United Nations Scientific Committee on the Effects of Atomic Radiation (UNSCEAR), 2010. Sources and Effects of Ionizing Radiation. UNSCEAR 2008 Report to the General Assembly, with Scientific Annexes. United Nations, New York.

Zhang, L., Wu, J., Guo, Q., Zhuo, W., 2010. Measurement of thoron gas in the environment using a Lucas scintillation cell. J. Radiol. Prot. 30, 597-605.

Figure captions

Figure 1 Measurement method of thoron and radon emanation. (a) Preparation of the sandwich sample. (b) Measurement system.

Figure 2 Growth curves of alpha counts or radon or thoron concentrations originating from the crushed uranium ore sample. (a) Scintillation cell. (b) RAD7. All points are experimental data, and solid lines are fitted curves. In the figure (a), the sum of the curves “Thoron” and “Radon” corresponds with that of “Total”. The uncertainties are identical to the standard deviations.

Figure 3 Theoretically determined curves of alpha counts with time for a sample with emanation rates of 1.6×10^{-4} for thoron and 2.7×10^{-8} Bq s^{-1} for radon in the scintillation-cell measurement. The experimental parameters (DL, $C_{\mathrm{BG,Rn\text{-}222}}$, and α) taken from the condition 1 (“Original”) in Table 2 were incorporated into the mathematical model of Table 1. The obtained activities were then converted to the counts according to Eqs. 1-3. At the initial time (t=0), it was assumed that radon concentration in the scintillation cell was the same as the background radon concentration in the laboratory ($C_{\mathrm{BG,Rn\text{-}222}}$=50 Bq m^{-3}), and that radon (existing in the cell volume) and its progeny (all deposited on the wall) were in equilibrium in the cell.

Figure 4 Expected relative uncertainties of thoron and radon emanation rates measured by the present method. The details of the experimental conditions are given in Table 2. The indicated reference values were calculated for the sample mass 2 g, which was typical for the dimension of the applied sandwich sample, using the world averages of radium concentrations and thoron and radon emanation fractions as indicated in the text.

Figure

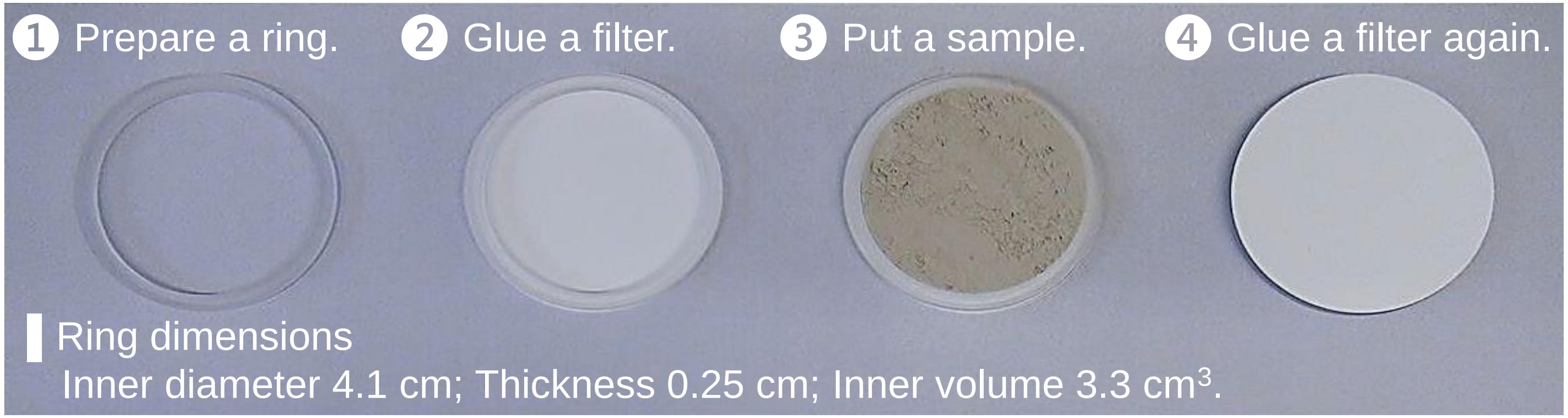

Figure 1 (a)

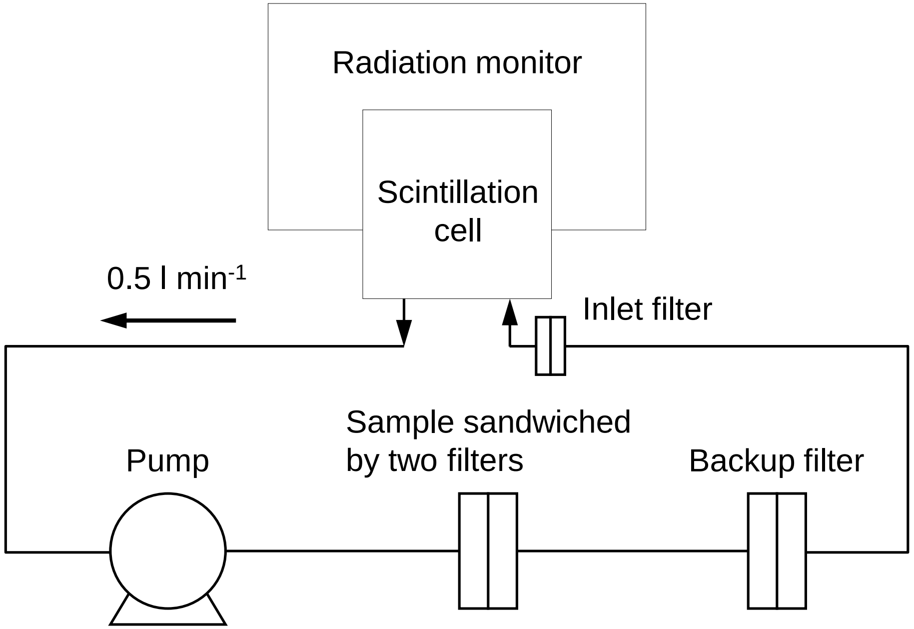

Figure 1 (b)

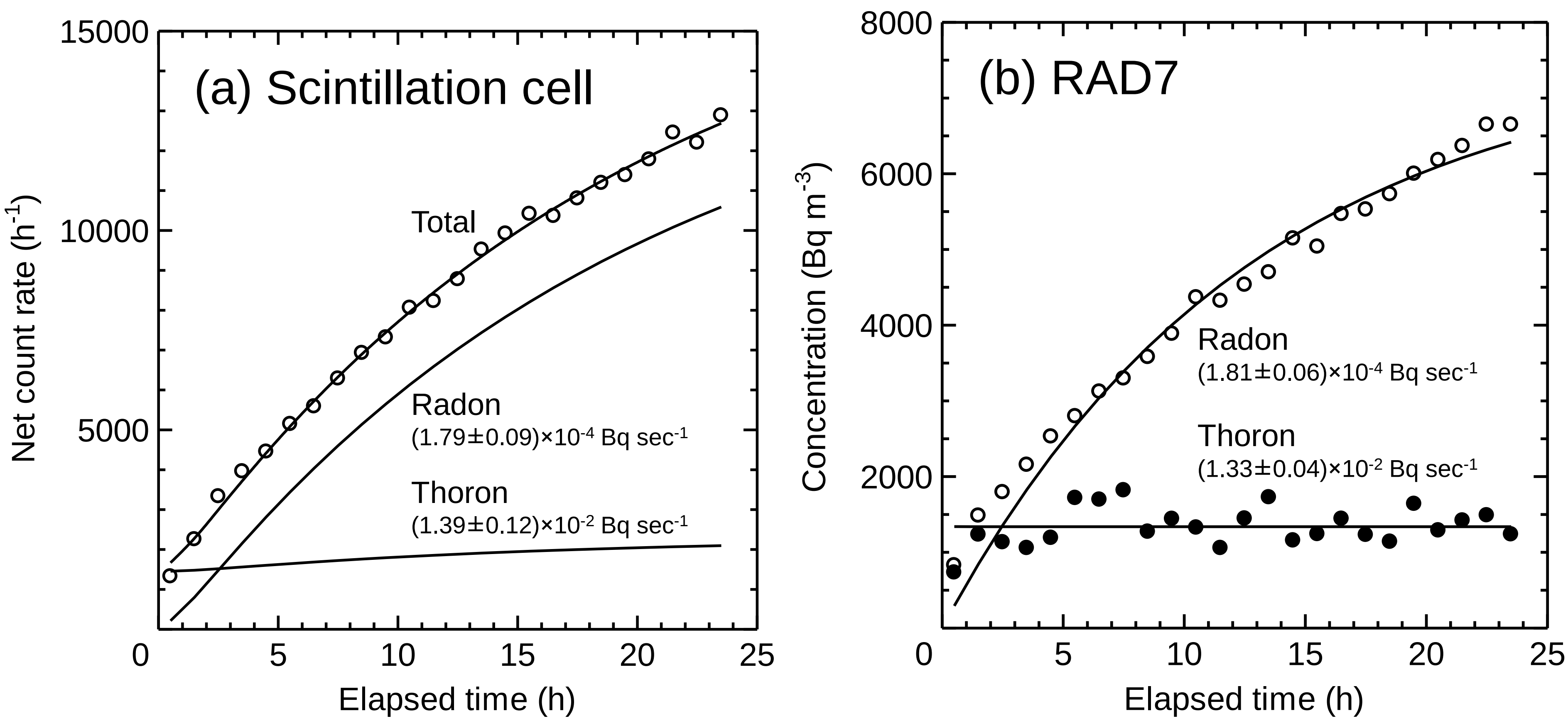
(a) Scintillation cell
Total
Radon
(1.79±0.09)×10-4 Bq sec-1
Thoron
(1.39±0.12)×10-2 Bq sec-1
Net count rate (h-1)
Elapsed time (h)
15000
10000
5000
0
5
10
15
20
25
(b) RAD7
Radon
(1.81±0.06)×10-4 Bq sec-1
Thoron
(1.33±0.04)×10-2 Bq sec-1
Concentration (Bq m-3)
Elapsed time (h)
8000
6000
4000
2000
0
5
10
15
20
25

Figure 2

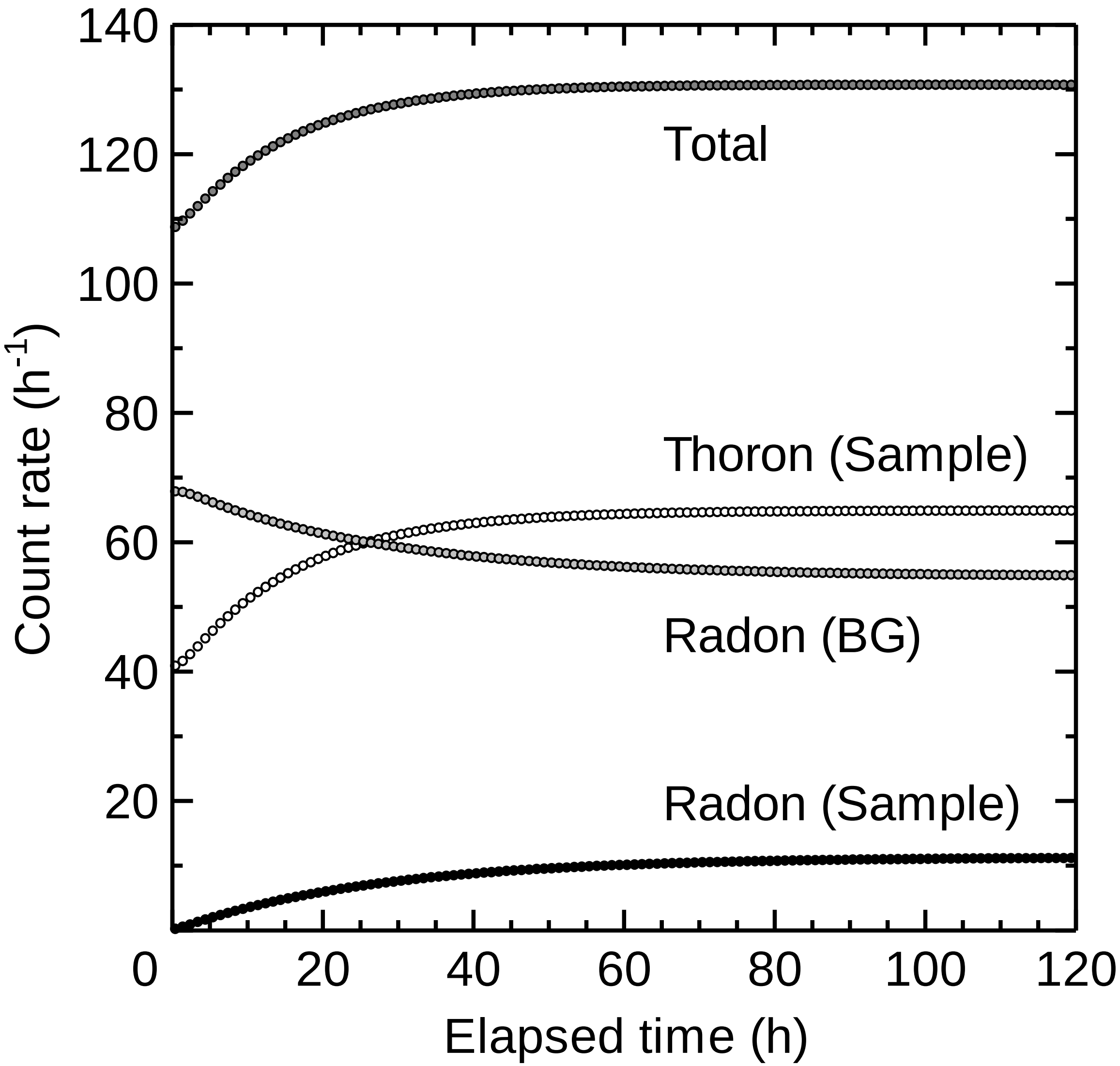

Count rate (h-1)
140
120
100
80
60
40
20
0
20
40
60
80
100
120
Elapsed time (h)
Total
Thoron (Sample)
Radon (BG)
Radon (Sample)

Figure 3

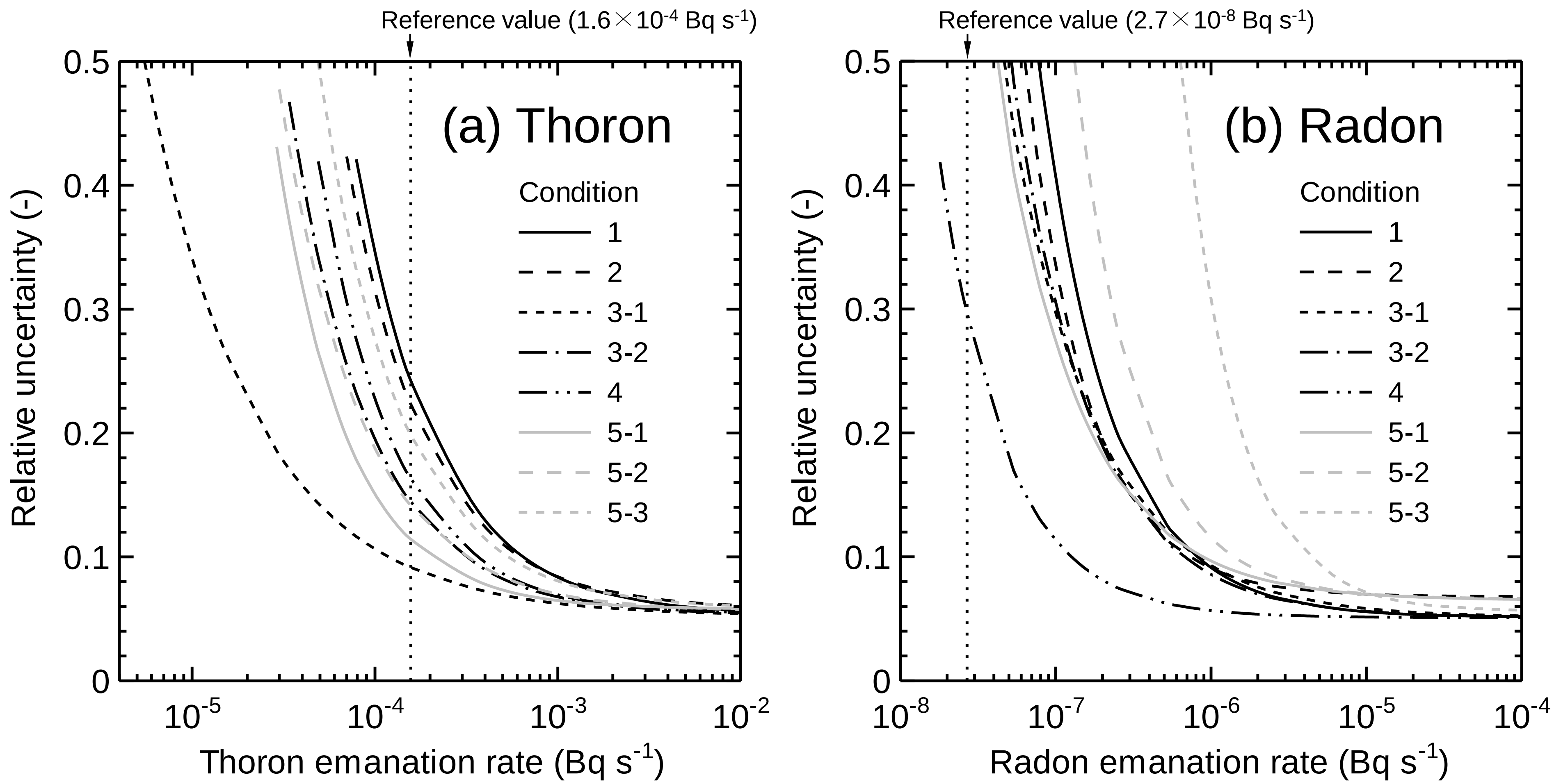

Reference value (1.6×10^-4 Bq s^-1)
(a) Thoron
Condition
1
2
3-1
3-2
4
5-1
5-2
5-3
Relative uncertainty (-)
Thoron emanation rate (Bq s^-1)
Reference value (2.7×10^-8 Bq s^-1)
(b) Radon
Condition
1
2
3-1
3-2
4
5-1
5-2
5-3
Relative uncertainty (-)
Radon emanation rate (Bq s^-1)

Figure 4

Table

Table 1 Mathematical model to determine the activities of thoron, radon and their progeny in the flow-through scintillation cell.

Series	Nuclide	Location of nuclide	Equation
Thoron	^{220}Rn (α decay)	In the cell volume	$\frac{\mathrm{d}A_{\mathrm{c,Rn\text{-}220}}}{\mathrm{d}t} = R_{\mathrm{Rn\text{-}220}} \mathrm{e}^{-\lambda_{\mathrm{Rn\text{-}220}} T_1} + \frac{v}{V} A_{\mathrm{c,Rn\text{-}220}} \mathrm{e}^{-\lambda_{\mathrm{Rn\text{-}220}} T_2} - \lambda_{\mathrm{Rn\text{-}220}} A_{\mathrm{c,Rn\text{-}220}} - \frac{v}{V} A_{\mathrm{c,Rn\text{-}220}}$
	^{216}Po (α decay)	In the cell volume	$A_{\mathrm{c,Po\text{-}216}} = A_{\mathrm{c,Rn\text{-}220}}$
	^{212}Pb	On the wall [b]	$\frac{\mathrm{d}A_{\mathrm{w,Pb\text{-}212}}}{\mathrm{d}t} = \varepsilon \lambda_{\mathrm{Pb\text{-}212}} A_{\mathrm{c,Po\text{-}216}} - \lambda_{\mathrm{Pb\text{-}212}} A_{\mathrm{w,Pb\text{-}212}}$
	^{212}Bi (α decay) [a]	On the wall [b]	$\frac{\mathrm{d}A_{\mathrm{w,Bi\text{-}212}}}{\mathrm{d}t} = \beta \lambda_{\mathrm{Bi\text{-}212}} A_{\mathrm{w,Pb\text{-}212}} - \lambda_{\mathrm{Bi\text{-}212}} A_{\mathrm{w,Bi\text{-}212}}$
	^{212}Po (α decay)	On the wall [b]	$A_{\mathrm{w,Po\text{-}212}} = \frac{1-\beta}{\beta} A_{\mathrm{w,Bi\text{-}212}}$
Radon	^{222}Rn (α decay)	In the cell volume	$\frac{\mathrm{d}A_{\mathrm{c,Rn\text{-}222}}}{\mathrm{d}t} = \frac{V}{V_{\mathrm{t}}} R_{\mathrm{Rn\text{-}222}} + \alpha V C_{\mathrm{BG,Rn\text{-}222}} - \lambda_{\mathrm{Rn\text{-}222}} A_{\mathrm{c,Rn\text{-}222}} - \alpha A_{\mathrm{c,Rn\text{-}222}}$
	^{218}Po (α decay)	In the cell volume	$\frac{\mathrm{d}A_{\mathrm{c,Po\text{-}218}}}{\mathrm{d}t} = (1-\varepsilon) \lambda_{\mathrm{Po\text{-}218}} A_{\mathrm{c,Rn\text{-}222}} - \lambda_{\mathrm{Po\text{-}218}} A_{\mathrm{c,Po\text{-}218}} - \frac{v}{V} A_{\mathrm{c,Po\text{-}218}}$
		On the wall	$\frac{\mathrm{d}A_{\mathrm{w,Po\text{-}218}}}{\mathrm{d}t} = \varepsilon \lambda_{\mathrm{Po\text{-}218}} A_{\mathrm{c,Rn\text{-}222}} - \lambda_{\mathrm{Po\text{-}218}} A_{\mathrm{w,Po\text{-}218}}$
	^{214}Pb	On the wall [b]	$\frac{\mathrm{d}A_{\mathrm{w,Pb\text{-}214}}}{\mathrm{d}t} = \lambda_{\mathrm{Pb\text{-}214}} A_{\mathrm{w,Po\text{-}218}} - \lambda_{\mathrm{Pb\text{-}214}} A_{\mathrm{w,Pb\text{-}214}}$
	^{214}Bi	On the wall [b]	$\frac{\mathrm{d}A_{\mathrm{w,Bi\text{-}214}}}{\mathrm{d}t} = \lambda_{\mathrm{Bi\text{-}214}} A_{\mathrm{w,Pb\text{-}214}} - \lambda_{\mathrm{Bi\text{-}214}} A_{\mathrm{w,Bi\text{-}214}}$
	^{214}Po (α decay)	On the wall [b]	$A_{\mathrm{w,Po\text{-}214}} = A_{\mathrm{w,Bi\text{-}214}}$

[a] The activity, $A_{\mathrm{w,Pb\text{-}212}}$, is taking into account alpha decay only.

[b] Based on our earlier data (Fig. 5 of Sakoda et al. (2015)), it was assumed that thoron progeny (^{212}Pb, ^{212}Bi and ^{212}Po) and radon progeny (^{214}Pb, ^{214}Bi and ^{214}Po) existing in the scintillation cell are all deposited on the cell wall in the flow condition.

Nomenclature: A (Bq) is the activity in the scintillation cell, R (Bq s^{-1}) the emanation rate of ^{220}Rn or ^{222}Rn from the material, λ (s^{-1}) the decay constant, T_1 and T_2 (s) the air-transfer times from the outlet of the cell to its inlet, and from the outlet of the sandwich sample to the inlet of the cell, respectively, v (m^3 s^{-1}) the flow rate, V and V_t (m^3) the inner cell volume and total volume of the measurement system, respectively, ε (-) the deposition fraction of ^{212}Pb or ^{218}Po onto the wall (Sakoda et al., 2015), α (s^{-1}) the leakage rate of ^{222}Rn from the measurement system, β (-) the branching ratio of ^{212}Bi to ^{208}Tl, and $C_{BG,Rn\text{-}222}$ (Bq m^{-3}) the background ^{222}Rn concentration outside the measurement system.

Table 2 Detection limits of thoron or radon emanation rates for different experimental conditions.

Experimental condition	Parameter [a]			Interest: Thoron		Interest: Radon	
	DL (MeV)	$C_{BG,Rn-222}$ (Bq m^{-3})	α (s^{-1})	Detection limit for thoron emanation (Bq s^{-1})	Assumed co-emanation for radon (Bq s^{-1}) [b]	Detection limit for radon emanation (Bq s^{-1})	Assumed co-emanation for thoron (Bq s^{-1}) [b]
(1) Original	4.0	50	8.3×10^{-6}	7.9×10^{-5}	2.7×10^{-8}	6.1×10^{-8}	1.6×10^{-4}
(2) Higher detection efficiency	1.2	50	8.3×10^{-6}	7.0×10^{-5}	2.7×10^{-8}	5.3×10^{-8}	1.6×10^{-4}
(3) No radon leakage	4.0	50	0	4.9×10^{-5}	2.7×10^{-8}	1.8×10^{-8}	1.6×10^{-4}
(4-1) Less background radon	4.0	10	8.3×10^{-6}	3.4×10^{-5}	2.7×10^{-8}	2.4×10^{-8}	1.6×10^{-4}
(4-2) No background radon	4.0	0	8.3×10^{-6}	4.9×10^{-6}	2.7×10^{-8}	1.7×10^{-8}	1.6×10^{-4}
(5-1) Lower activity	1.2	10	8.3×10^{-6}	2.9×10^{-5}	2.7×10^{-8}	2.0×10^{-8}	1.6×10^{-4}
(5-2) Intermediate activity	1.2	10	8.3×10^{-6}	3.0×10^{-5}	2.7×10^{-7}	7.7×10^{-8}	1.6×10^{-3}
(5-3) Higher activity	1.2	10	8.3×10^{-6}	4.7×10^{-5}	2.7×10^{-6}	4.7×10^{-7}	1.6×10^{-2}

[a] *DL* stands for the discrimination level for alpha counting with the scintillation cell, $C_{BG,Rn-222}$ the background radon concentration outside the measurement system (i.e. air in the laboratory), α is the leakage rate of radon from the measurement system. The condition "Original" is the usual experimental condition seen in the present study.

[b] *Co-emanation* is the co-existing radon or thoron emanation which is not of interest there (see the text for the details). The co-emanation rates of radon (2.7×10^{-8} Bq s^{-1}) and thoron (1.6×10^{-4} Bq s^{-1}) were assumed in terms of world averages: the ^{226}Ra and ^{224}Ra activities are 32 and 45 Bq kg^{-1} (UNSCEAR, 2010), respectively, the radon and thoron emanation fractions are 0.2 (Sakoda et al., 2011) and 0.14 (IAEA, 2013), respectively, and the sample mass is 2 g (typical for the dimension of the present sandwich sample). The co-emanation rate can be calculated by multiplying the product of these three parameters with the decay constant of radon or thoron.

Table 3 Detection efficiencies of alpha particles from thoron, radon and their progeny in the scintillation cell.

Discrimination level (MeV)	Calculated detection efficiency (-)						
	^{220}Rn (cell)	^{216}Po (cell)	^{212}Bi (wall)	^{212}Po (wall)	^{222}Rn (cell)	^{218}Po (cell/wall)	^{214}Po (wall)
1.2	0.738±0.043	0.810±0.027	0.708±0.026	0.888±0.003	0.618±0.055	0.703±0.047 / 0.704±0.026	0.856±0.010
4.0	0.465±0.036	0.583±0.032	0.592±0.013	0.853±0.007	0.304±0.040	0.415±0.037 / 0.589±0.013	0.731±0.014

Note: The values were calculated by Monte Carlo simulation, for the two different discrimination levels for alpha counting (see Sakoda et al. (2015) for the details). Detection efficiencies similar to those given by the *DL* of 1.2 MeV have usually been used in some other studies (e.g. Sakoda et al., 2015; Zhang et al., 2010; Tokonami et al., 2002).